Super-convergence of Reproducing Kernel Approximation

Yu Leng[a], Xiaochuan Tian[b], John T. Foster[a]

[a] *Department of Petroleum and Geosystems Engineering, The University of Texas at Austin, Austin, TX 78712*
[b] *Department of Mathematics, The University of Texas at Austin, Austin, TX 78712*

Abstract

The reproducing kernel particle methods (RKPM) are meshfree methods arising in mechanics, especially in dealing with problems involving large deformation and singularities. We provide a theoretical analysis of super-convergence in Sobolev norms for reproducing kernel (RK) approximations when the interpolation order p is even. Super-convergence phenomenon means the convergence rate is higher than the order that is generally expected. We distinguish the continuous RK approximation and the discrete RKP approximation. While the continuous RK approximations are proven to be super-convergent when p is even, its discrete counterpart has super-convergence only with uniform particle distribution and special choices of RK kernel functions and support sizes. Super-convergence does not exist for the discrete RKP approximation with general RK support sizes. At last, the concept of pseudo-super-convergence is introduced to explain why in practice the super-convergence phenomenon is sometimes observed for general cases although in theory it is not true. Our analysis is general for multi-dimensional RK approximations.

1. Introduction

The reproducing kernel (RK) approximation of functions introduced by [17] uses integral transformation with corrected kernel functions, which are determined by the reproducing conditions. The reproducing kernel particle methods (RKPM) ([8, 17]) are meshfree methods based on RK approximations. RKPM has attracted many attentions from researchers to use this method to solve partial differential equations in Galerkin procedure. It is especially effective for problems with large deformations ([7, 9, 15]). Recently, people have used RKPM to solve nonlocal peridynamics models ([14]).

The conventional error estimates of RKPM in [5] and [18] yield same order of convergence as in classical finite element methods. Many numerical experiments (see e.g. [10, 14]), however, show that these error estimates are rather conservative and super-convergence rates have been observed for even order RKPM. A synchronized convergence phenomenon is introduced in [10] and its applications are exploited in [4, 11, 12, 13]. Their interest is to achieve the same order of convergence rate in high-order error norms as in L^2 error norm in the interior of the domain. To achieve the synchronized convergence, a crucial requirement is that the correction function to be a constant in the interior of the domain. This condition, to the knowledge of the authors, is rather restrictive and it is shown to be possible in the literature only when interpolation order p is 1. In this work, we will show that the convergence rate under all Sobolev norms can be improved for all even order RK approximations over the entire computation domain. For convenience, when we say even order RK approximation we actually refer to RK approximation with even order interpolation, i.e., p is even. We will mainly use the analytic tool in [10], but our concerns are completely different from the synchronized convergence phenomenon. In this work, we provide the theoretical analysis of the super-convergence phenomena, which is based on the observation that in the interior of domain, the RK shape function of even order basis is in fact identical to the shape function of one order higher. Error estimates in Sobolev spaces are given in this work for both the RK approximations and the RKP approximations. For convenience, we will call the RK integral approximation of functions as the *continuous RK approximation*, and the RKP approximation using particles the *discrete RK approximation*. Although in practice integrals are always replaced by finite sums, the discussion of continuous RK approximation followed by its discrete counterpart in this paper bears the significance of helping us to see in a clear way the origin of the super-convergence phenomena. It turns out that the discrete RKP approximation is super-convergent with even interpolation order p only when the window function satisfies the Strang-Fix condition. This can be achieved, for instance, by choosing B-spline functions to be the window function with RK support size selected wisely. However, when the RK support size is arbitrary, super-convergence is sometimes observed in numerical experiments within certain range of numerical resolutions. We will use numerical examples to explain that the in the case of arbitrary RK support size, the super-convergence is not true for all scales of numerical solutions. We thus call it a phenomenon of pseudo-super-convergence.

This paper is organized as follows. Section 2 introduces the continuous and discrete RK approximations. Super-convergence for continuous RK

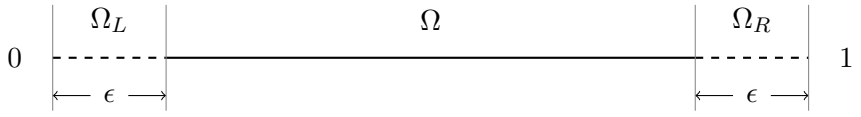

Figure 1: Domain decomposition in 1d. $\overline{\overline{\Omega}} = \Omega_{bl} \cup \Omega$ and $\Omega_{bl} = \Omega_L \cup \Omega_R$

approximation is shown in Section 3 and this lays the foundation on the analysis of super-convergence for RK approximations. In Section 4, super-convergence for discrete RK approximation with selected RK support sizes is presented. To better demonstrate the analysis, we work on one dimension in Sections 2-4. The multi-dimensional extension is then natural and is presented in Section 5. Numerical experiments that verify the super-convergence of discrete RK approximation are presented in Section 6. Then the discussion of discrete RK approximation with arbitrary RK support size is in Section 7, where the concept of pseudo-super-convergence is introduced. Finally, conclusions are made in Section 8.

2. RK approximation

The continuous RK approximation of functions uses integral transformation with corrected kernel functions. In practice, integrals are replaced by finite summations, which leads to discrete RK approximations. The corrected kernel functions are determined by the reproducing conditions. Therefore RK approximations exactly reproduce polynomials. We will review the notations of the continuous and discrete RK approximation in Sections 2.1 and 2.2 respectively.

In this section and the following two sections, we will work on the 1d domain $\overline{\overline{\Omega}} \subset \mathbb{R}$. The generalization to multi-dimension is natural and will be discussed in Section 5. In Figure 1, the domain of interest is given by $\overline{\overline{\Omega}} = (0, 1)$ and the interior of the domain is defined by $\Omega = (\epsilon, 1 - \epsilon)$, where ϵ is a parameter in the RK approximation that will be introduced shortly. Notice that the boundary of the domain $\overline{\overline{\Omega}}$ (denoted by $\Omega_{bl} = \overline{\overline{\Omega}} \backslash \Omega$) is not the usual codimension one boundary, but rather a boundary layer of width ϵ inside $\overline{\overline{\Omega}}$. The main idea of the error analysis in the following sections is to investigate the approximation errors separately on the interior Ω and on the boundary layer Ω_{bl}.

2.1. Continuous RK approximation

For a small number $\epsilon > 0$, $u_\epsilon(x)$ is the RK approximation of a given function $u(x)$ on $\overline{\overline{\Omega}}$ defined by

$$u_\epsilon(x) = \int_{\overline{\overline{\Omega}}} \widetilde{\Psi}_\epsilon(x; x-y) u(y) dy \,, \tag{1}$$

where $\widetilde{\Psi}_\epsilon(x; x-y)$ is the modified kernel function given by

$$\widetilde{\Psi}_\epsilon(x; x-y) = C(x; x-y)\phi_\epsilon(x-y) \,. \tag{2}$$

$C(x; x-y)$ is the correction function obtained by imposing the reproducing conditions such that the RK approximation exactly reproduces polynomials. $\phi_\epsilon(x-y)$ is the kernel function given by

$$\phi_\epsilon(x) = \frac{1}{\epsilon}\phi\left(\frac{x}{\epsilon}\right), \tag{3}$$

where $\phi(x)$ is a symmetric nonnegative function supported on $[-1, 1]$, which we call the *window function*. Notice that we do not require the integral of the kernel function ϕ to be 1 since any scaling factor can be absorbed into the correction function. Now for p being a nonnegative integer, the correction function $C(x; x-y)$ is given by

$$C(x; x-y) = \boldsymbol{H}_p^T(x-y)\boldsymbol{b}_p(x), \tag{4}$$

where $\boldsymbol{H}_p^T(x-y)$ is a row vector consisting of monomial basis functions of degree p:

$$\boldsymbol{H}_p^T(x-y) = [1, x-y, (x-y)^2, \cdots, (x-y)^p] \,.$$

$\boldsymbol{b}_p(x)$ is a column vector containing correction function coefficients obtained from the p-th order reproducing condition:

$$\int_{\overline{\overline{\Omega}}} \widetilde{\Psi}_\epsilon(x; x-y) y^\alpha dy = x^\alpha, \quad \alpha = 0, 1, \ldots, p, \tag{5}$$

which is equivalent to

$$\int_{\overline{\overline{\Omega}}} \widetilde{\Psi}_\epsilon(x; x-y) \boldsymbol{H}_p(x-y) dy = \boldsymbol{H}_p(0). \tag{6}$$

Substitute equations (2) and (4) into (6) we obtain

$$\widetilde{\boldsymbol{M}}_p(x)\boldsymbol{b}_p(x) = \boldsymbol{H}_p(0), \tag{7}$$

where

$$\widetilde{\boldsymbol{M}}_p(x) = \int_{\overline{\overline{\Omega}}} \boldsymbol{H}_p(x-y)\phi_\epsilon(x-y)\boldsymbol{H}_p^T(x-y)dy, \tag{8}$$

is a $(p+1)\times(p+1)$ matrix and is called moment matrix. Denote $\widetilde{\boldsymbol{M}}(x) = (\widetilde{M}_{ij}(x))_{i,j=0}^{p}$, then each entry $\widetilde{M}_{ij}$ is the $(i+j)$-th moment of ϕ_ϵ given by

$$\widetilde{M}_{ij}(x) = \widetilde{m}_{i+j}(x) := \int_{\overline{\overline{\Omega}}} (x-y)^{i+j}\phi_\epsilon(x-y)dy, \quad 0 \le i,j \le p. \tag{9}$$

$\boldsymbol{b}_p(x)$ is then obtained by solving the system of equation (7):

$$\boldsymbol{b}_p(x) = \widetilde{\boldsymbol{M}}_p^{-1}(x)\boldsymbol{H}_p(0). \tag{10}$$

By combining equations (2), (4), and (10), we obtain the modified kernel function

$$\widetilde{\Psi}_\epsilon(x; x-y) = \boldsymbol{H}_p^T(x-y)\widetilde{\boldsymbol{M}}_p^{-1}(x)\boldsymbol{H}_p(0)\phi_\epsilon(x-y). \tag{11}$$

2.2. Discrete RK approximation

For practical computations, integrals are replaced by summations. Suppose the domain $\overline{\overline{\Omega}}$ is discretized into a total number of I nodes $\{x_k\}_{k=1}^{I}$, the discrete RK approximation is then a numerical approximation of equation (1):

$$u(x) \approx u^I(x) = \sum_{k=1}^{I} \Psi_k(x)u(x_k)\,, \tag{12}$$

where the modified kernel function $\Psi_k(x)$ is defined by

$$\Psi_k(x) = C(x, x-x_k)\phi_\epsilon(x-x_k)\,. \tag{13}$$

$\Psi_k(x)$ is also referred to as the *RK shape function* in the literature. Notice that equation (12) does not contain any quadrature weights because they can be absorbed into the shape function. The p-th order reproducing condition is then replaced by the discrete reproducing condition:

$$\sum_{k=1}^{I} \Psi_k(x)x_k^\alpha = x^\alpha, \quad \alpha = 0, 1, \ldots, p. \tag{14}$$

which is equivalent to

$$\sum_{k=1}^{I} \Psi_k(x) \boldsymbol{H}_p(x - x_k) = \boldsymbol{H}_p(0). \tag{15}$$

Substitute equations (13) and (4) into (15) we obtain

$$\boldsymbol{M}_p(x)\boldsymbol{b}_p(x) = \boldsymbol{H}_p(0),$$

where $\boldsymbol{M}_p = (M_{ij})_{i,j=0}^{p}$ is the discrete moment matrix given by

$$\boldsymbol{M}_p(x) = \sum_{k=1}^{I} \boldsymbol{H}_p(x - x_k)\phi_\epsilon(x - x_k)\boldsymbol{H}_p^T(x - x_k)\,. \tag{16}$$

Each entry $M_{ij}(x)$ is the $(i + j)$-th discrete moment:

$$M_{ij}(x) = m_{i+j}(x) := \sum_{k=1}^{I} (x - x_k)^{i+j}\phi_\epsilon(x - x_k), \quad 0 \le i, j \le p\,. \tag{17}$$

Similar to equation (10), we now have

$$\boldsymbol{b}_p(x) = (\boldsymbol{M}_p)^{-1}(x)\boldsymbol{H}_p(0). \tag{18}$$

By substituting equations (4) and (18) into (13), the RK shape function is obtained as

$$\Psi_k(x) = \boldsymbol{H}_p^T(x - x_k)(\boldsymbol{M}_p)^{-1}(x)\boldsymbol{H}_p(0)\phi_\epsilon(x - x_k),\ k = 1, \cdots, I\,. \tag{19}$$

We call $u^I(x)$ the RK interpolant of $u(x)$. Note that $u^I(x_k)$ is usually not agreed with $u(x_k)$, so $u^I(x)$ is viewed an interpolant of $u(x)$ in a generalized sense.

3. Super-convergence for continuous RK approximation

The error estimates for the RK approximation are done using Taylor expansion (see [5, 18]). We first give a brief review of them for completeness. Notice that we focus on the continuous RK approximation in this section. To give estimates in Sobolev space, we will need the so called averaged Taylor polynomial, since derivatives may not exist in the pointwise sense. As in [5], we use the notation $W^{p,q}$ for Sobolev space, where p is the order of derivative and q denotes the L^q norm.

Now suppose that the whole domain $\overline{\overline{\Omega}}$ has a finite cover $\cup_{j=1}^{N(\epsilon)} B_j$, where each set B_j is a ball of diameter ϵ and each point $x \in \overline{\overline{\Omega}}$ is covered by at most a fixed number of sets in $\{B_j\}_{j=1}^{N(\epsilon)}$. Define

$$\hat{B}_j = \{x : \mathrm{dist}(x, B_j) < \epsilon\},$$

then $\cup_{j=1}^{N(\epsilon)} \hat{B}_j$ is again a covering of $\overline{\overline{\Omega}}$. Assume that each point $x \in \overline{\overline{\Omega}}$ is covered by at most K_0 sets in $\{\hat{B}_j\}_{j=1}^{N(\epsilon)}$, where K_0 is a constant independent of ϵ. This can be satisfied, for instance, by choosing $\{B_j\}_{j=1}^{N(\epsilon)}$ to a collection of uniformly distributed balls over the domain $\overline{\overline{\Omega}}$. Note that the finite cover has nothing to do with the discretization of the domain $\overline{\overline{\Omega}}$. The error estimate is done locally on each set $B_j \cap \overline{\overline{\Omega}}$. Let $Q_j^p u(x)$ be the Taylor polynomial of degree p of u averaged over B_j (see [1, 3]), and denote the remainder

$$R_j^p u(x) = u(x) - Q_j^p u(x), \quad \forall x \in B_j \cap \overline{\overline{\Omega}}.$$

Then from the results of [1, Section 4.3], we have the following estimates

$$\|R_j^p u\|_{L^\infty(\hat{B}_j \cap \overline{\overline{\Omega}})} \leq C\epsilon^{p+1-1/q} \|u\|_{W^{p+1,q}(\hat{B}_j \cap \overline{\overline{\Omega}})}, \quad \text{and} \tag{20}$$

$$\|R_j^p u\|_{W^{l,q}(\hat{B}_j \cap \overline{\overline{\Omega}})} \leq C\epsilon^{p+1-l} \|u\|_{W^{p+1,q}(\hat{B}_j \cap \overline{\overline{\Omega}})} \quad \text{for } l = 0, 1, \cdots, p+1, \tag{21}$$

where C only depends on p and q. Notice that in multi-dimension, the power on ϵ in (20) becomes $p + 1 - d/q$ and that (21) is a constructive form of the Bramble-Hilbert lemma. Now for $x \in B_j \cap \overline{\overline{\Omega}}$, we can write by applying (1) that

$$\begin{aligned} u(x) - u_\epsilon(x) =& Q_j^p u(x) - \int_{\overline{\overline{\Omega}}} \widetilde{\Psi}_\epsilon(x; x-y) Q_j^p u(y) dy \\ &+ R_j^p u(x) - \int_{\overline{\overline{\Omega}}} \widetilde{\Psi}_\epsilon(x; x-y) R_j^p u(y) dy. \end{aligned}$$

Since $Q_j^p u(x)$ is a polynomial of degree p, we have by the reproducing condition (5) that

$$Q_j^p u(x) = \int_{\overline{\overline{\Omega}}} \widetilde{\Psi}_\epsilon(x; x-y) Q_j^p u(y) dy, \quad \forall x \in B_j \cap \overline{\overline{\Omega}}. \tag{22}$$

Thus

$$u(x) - u_\epsilon(x) = R_j^p u(x) - \int_{\overline{\overline{\Omega}}} \widetilde{\Psi}_\epsilon(x; x-y) R_j^p u(y) dy \,,$$

for $x \in B_j \cap \overline{\overline{\Omega}}$ and then

$$\begin{aligned} \|u - u_\epsilon\|_{W^{l,q}(B_j \cap \overline{\overline{\Omega}})} &\le \|R_j^p u\|_{W^{l,q}(B_j \cap \overline{\overline{\Omega}})} \\ &+ \|R_j^p u\|_{L^\infty(\hat{B}_j \cap \overline{\overline{\Omega}})} \sum_{k=0}^{l} \| \int_{\overline{\overline{\Omega}}} \left| D_x^k \widetilde{\Psi}_\epsilon(x; x-y) \right| dy \|_{L^q(B_j \cap \overline{\overline{\Omega}})} \,, \end{aligned} \tag{23}$$

where D_x^k stands for the k-th derivative with respect to x. Notice that the support of $\widetilde{\Psi}_\epsilon(x; x-y)$ is $y \in B_\epsilon(x)$ and by the calculations of [18, Lemma 2.1], one has

$$D_x^k C(x; x-y) = O(\epsilon^{-k}), \quad \text{for } y \in B_\epsilon(x) \,,$$

if the window function ϕ is k-th continuously differentiable. So we can obtain by (2) that

$$D_x^k \widetilde{\Psi}_\epsilon(x; x-y) = O(\epsilon^{-k-1}), \quad \text{for } y \in B_\epsilon(x) \,. \tag{24}$$

Now substitute equations (20), (21) and (24) into (23), we obtain

$$\|u - u_\epsilon\|_{W^{l,q}(B_j \cap \overline{\overline{\Omega}})} \le C\epsilon^{p+1-l} \|u\|_{W^{p+1,q}(\hat{B}_j \cap \overline{\overline{\Omega}})} \,, \tag{25}$$

for all $l = 0, 1, \cdots, p+1$. Therefore we conclude that

$$\begin{aligned} \|u - u_\epsilon\|_{W^{l,q}(\overline{\overline{\Omega}})} &\le \sum_{j=1}^{N(\epsilon)} \|u - u_\epsilon\|_{W^{l,q}(B_j \cap \overline{\overline{\Omega}})} \le C\epsilon^{p+1-l} \sum_{j=1}^{N(\epsilon)} \|u\|_{W^{p+1,q}(\hat{B}_j \cap \overline{\overline{\Omega}})} \\ &\le \tilde{C}\epsilon^{p+1-l} \|u\|_{W^{p+1,q}(\overline{\overline{\Omega}})} \,, \quad l = 0, 1, \cdots p+1 \,, \end{aligned} \tag{26}$$

where $\tilde{C} = CK_0$, and the last step in (26) is by that fact that $x \in \overline{\overline{\Omega}}$ is covered by at most K_0 sets in $\{\hat{B}_j\}_{j=1}^{N(\epsilon)}$.

The previous lines of arguments and the final estimate (26) share the same idea with [5] and [18], although details may differ. Equation (26) tells us that the RK approximation of p-th order can achieve at most $p+1$-th order convergence in L^2 norm provided that the function u is in the Sobolev space $W^{p+1,2}$. However, many numerical experiments (see [10, 14]) have

shown that super-convergence exists for even order RK basis (p is an even number).

In the following, we provide careful error analysis that explains the super-convergence phenomena for p being an even number. The basic idea is to investigate the errors in the interior and boundary of the domain separately. We will show that a p-th order RK approximation can actually achieve $(p+1)$-th reproducing condition in the interior of the domain if p is an even number. This fact is the key to obtain the super-convergence result as we have seen that equation (22) relies totally on the reproducing condition. We begin with a lemma that characterizes the moment function $\widetilde{m}_\alpha(x)$ in the interior of the domain.

Lemma 3.1. *For $x \in \Omega$, the moment $\widetilde{m}_\alpha(x) = 0$ if α is an odd number.*

Proof. Recall that $\widetilde{m}_\alpha(x)$ is defined by equation (9). First notice that for $x \in \Omega$, we have $B_\epsilon(x)$ fully contained in $\overline{\overline{\Omega}}$. Since kernel function $\phi_\epsilon(z)$ is symmetric, it implies that for any $x \in \Omega$, $\widetilde{m}_\alpha(x)$ is zero when α is an odd number. □

Lemma 3.1 is simple enough by observation, but it leads to the following crucial property for the correction coefficients vector.

Lemma 3.2. *Let $\boldsymbol{b}_p(x) = \widetilde{\boldsymbol{M}}_p^{-1}(x)\boldsymbol{H}_p(0)$ and let $b_p^{(i)}$ $(0 \le i \le p)$ be the components of $\boldsymbol{b}_p$. In the interior of the domain $(x \in \Omega)$, we have*

(a) $b_p^{(i)}(x) = 0$ for i being an odd number, and

(b) $b_p^{(i)}(x) = b_{p+1}^{(i)}(x)$ for $p = 2k$, where $k \in \mathbb{N}$.

Proof. We are going to show (a) first. Here we always assume that $x \in \Omega$ and we drop the x-dependence of the vectors for convenience. The proof of (a) contains two cases where p is even or odd. For p being an even number, we assume that $p = 2k$, where $k \in \mathbb{N}$. Since all the odd order moments vanish by Lemma 3.1, equation (7) becomes

$$\begin{bmatrix} \widetilde{m}_0 & 0 & \cdots & \widetilde{m}_{2k} \\ 0 & \widetilde{m}_2 & \cdots & 0 \\ \vdots & \vdots & \ddots & \vdots \\ \widetilde{m}_{2k} & 0 & \cdots & \widetilde{m}_{4k} \end{bmatrix} \begin{bmatrix} b_{2k}^{(0)} \\ b_{2k}^{(1)} \\ \vdots \\ b_{2k}^{(2k)} \end{bmatrix} = \begin{bmatrix} 1 \\ 0 \\ \vdots \\ 0 \end{bmatrix}, \tag{27}$$

which can be written into two independent systems based on even and odd rows of $\boldsymbol{b}_{2k}$:

$$\begin{bmatrix} \widetilde{m}_0 & \widetilde{m}_2 & \cdots & \widetilde{m}_{2k} \\ \widetilde{m}_2 & \widetilde{m}_4 & \cdots & \widetilde{m}_{2k+2} \\ \vdots & \vdots & \ddots & \vdots \\ \widetilde{m}_{2k} & \widetilde{m}_{2k+2} & \cdots & \widetilde{m}_{4k} \end{bmatrix} \begin{bmatrix} b_{2k}^{(0)} \\ b_{2k}^{(2)} \\ \vdots \\ b_{2k}^{(2k)} \end{bmatrix} = \begin{bmatrix} 1 \\ 0 \\ \vdots \\ 0 \end{bmatrix}, \tag{28}$$

and

$$\begin{bmatrix} \widetilde{m}_2 & \widetilde{m}_4 & \cdots & \widetilde{m}_{2k} \\ \widetilde{m}_4 & \widetilde{m}_6 & \cdots & \widetilde{m}_{2k+2} \\ \vdots & \vdots & \ddots & \vdots \\ \widetilde{m}_{2k} & \widetilde{m}_{2k+2} & \cdots & \widetilde{m}_{4k-2} \end{bmatrix} \begin{bmatrix} b_{2k}^{(1)} \\ b_{2k}^{(3)} \\ \vdots \\ b_{2k}^{(2k-1)} \end{bmatrix} = \begin{bmatrix} 0 \\ 0 \\ \vdots \\ 0 \end{bmatrix}. \tag{29}$$

Since the moment matrix is a Gram matrix which is invertible ([18]), it is apparent that the matrices in the two linear systems (28) and (29) are also invertible. So the solution to equation (29) is $\mathbf{0}$, i.e. $b_{2k}^{(i)}(x) = 0$ for i being an odd number.

For the second case where $p = 2k+1, k \in \mathbb{N}$, follow the same procedure as before we have

$$\begin{bmatrix} \widetilde{m}_0 & 0 & \cdots & \widetilde{m}_{2k} & 0 \\ 0 & \widetilde{m}_2 & \cdots & 0 & \widetilde{m}_{2k+2} \\ \vdots & \vdots & \ddots & \vdots & \vdots \\ \widetilde{m}_{2k} & 0 & \cdots & \widetilde{m}_{4k} & 0 \\ 0 & \widetilde{m}_{2k+2} & \cdots & 0 & \widetilde{m}_{4k+2} \end{bmatrix} \begin{bmatrix} b_{2k+1}^{(0)} \\ b_{2k+1}^{(1)} \\ \vdots \\ b_{2k+1}^{(2k)} \\ b_{2k+1}^{(2k+1)} \end{bmatrix} = \begin{bmatrix} 1 \\ 0 \\ \vdots \\ 0 \\ 0 \end{bmatrix}. \tag{30}$$

Rewrite equation (30) into the two independent systems

$$\begin{bmatrix} \widetilde{m}_0 & \widetilde{m}_2 & \cdots & \widetilde{m}_{2k} \\ \widetilde{m}_2 & \widetilde{m}_4 & \cdots & \widetilde{m}_{2k+2} \\ \vdots & \vdots & \ddots & \vdots \\ \widetilde{m}_{2k} & \widetilde{m}_{2k+2} & \cdots & \widetilde{m}_{4k} \end{bmatrix} \begin{bmatrix} b_{2k+1}^{(0)} \\ b_2^{2k+1} \\ \vdots \\ b_{2k+1}^{(2k)} \end{bmatrix} = \begin{bmatrix} 1 \\ 0 \\ \vdots \\ 0 \end{bmatrix}, \tag{31}$$

and

$$\begin{bmatrix} \widetilde{m}_2 & \widetilde{m}_4 & \cdots & \widetilde{m}_{2k+2} \\ \widetilde{m}_4 & \widetilde{m}_6 & \cdots & \widetilde{m}_{2k+4} \\ \vdots & \vdots & \ddots & \vdots \\ \widetilde{m}_{2k} & \widetilde{m}_{2k+2} & \cdots & \widetilde{m}_{4k} \\ \widetilde{m}_{2k+2} & \widetilde{m}_{2k+4} & \cdots & \widetilde{m}_{4k+2} \end{bmatrix} \begin{bmatrix} b_{2k+1}^{(1)} \\ b_{2k+1}^{(3)} \\ \vdots \\ b_{2k+1}^{(2k-1)} \\ b_{2k+1}^{(2k+1)} \end{bmatrix} = \begin{bmatrix} 0 \\ 0 \\ \vdots \\ 0 \\ 0 \end{bmatrix}. \tag{32}$$

Equation (32) has only the trivial solution, i.e., $b_{2k+1}^{(i)} = 0$ for i being an odd number. Combine the two cases, (a) is shown.

Now observe that the coefficient matrices in equations (31) and (28) are exactly the same, therefore their solutions are identical, i.e., $b_{2k+1}^{(i)} = b_{2k}^{(i)}$, for $i = 2n, n \in \mathbb{N}$. This completes the proof of (b). □

By the result of Lemma 3.2, we can identify the modified kernel function $\widetilde{\Psi}_\epsilon$ of an even order to the that of an odd order. For convenience we denote $\widetilde{\Psi}_\epsilon(p, x; x - y)$ to be the modified kernel function with respect to the RK approximation of p-th order, then we have the following result.

Lemma 3.3. *If p is even, then the modified kernel functions of p-th and $(p+1)$-th order are identical in the interior of the domain, that is*

$$\widetilde{\Psi}_\epsilon(p, x; x - y) = \widetilde{\Psi}_\epsilon(p+1, x; x - y), \quad x \in \Omega.$$

Proof. If p is even, use Lemma 3.2, we have for $x \in \Omega$ that

$$\boldsymbol{b}_{p+1}^T(x) = [\boldsymbol{b}_p^T(x), \ \ 0].$$

Then by equations (2) and (4) we have obviously that $\widetilde{\Psi}_\epsilon(p, x; x - y)$ and $\widetilde{\Psi}_\epsilon(p+1, x; x - y)$ are identical. □

Lemma 3.3 essentially says that for even number p, the p-th order RK approximation can achieve $(p+1)$-th reproducing condition in the interior of the domain, which is crucial in proving super-convergence. When showing

the final theorem, we need functions to be approximated free from pathological behavior in the boundary layer. More specially, we want that the Sobolev norm of a function u has uniform density in the boundary layer and in the interior of the domain. We thus give the following definition.

Definition 3.4. *Suppose that* $\overline{\overline{\Omega}} \subset \mathbb{R}^d$, *and* $\Omega_{bl} = \{x \in \overline{\overline{\Omega}} : dist(x, \partial\Omega) < \epsilon\}$. *We say that a function* $u \in W^{p,q}(\overline{\overline{\Omega}})$ *is proper if*

$$\|u\|_{W^{p,q}(\Omega_{bl})} \leq C\epsilon^{d/q}\|u\|_{W^{p,q}(\overline{\overline{\Omega}})}. \tag{33}$$

One can easily check that if $u \in W^{p,q}(\overline{\overline{\Omega}}) \cap C^p(\overline{\overline{\Omega}})$, then equation (33) is satisfied.

We now go back to the 1d case and show the convergence theorem for the continuous RK approximation.

Theorem 3.5. *Assume that the window function* $\phi \in C^{p+2}$, *and* $u \in W^{p+2,q}(\overline{\overline{\Omega}})$ *is proper. Then the error estimate for the continuous RK approximation is as follows:*
if p *is odd,*

$$\|u - u_\epsilon\|_{W^{l,q}(\overline{\overline{\Omega}})} \leq C\epsilon^{p+1-l}\|u\|_{W^{p+1,q}(\overline{\overline{\Omega}})},$$

and if p *is even,*

$$\|u - u_\epsilon\|_{W^{l,q}(\overline{\overline{\Omega}})} \leq C\epsilon^{p+1+1/q-l}\|u\|_{W^{p+2,q}(\overline{\overline{\Omega}})},$$

for $l = 0, 1, \cdots p+1$.

Proof. If p is an odd number, the error estimate is the same one as equation (26) shows. Now assume that p is even, then we divide the domain $\overline{\overline{\Omega}}$ into two parts, as shown in Figure (1), and investigate approximation errors on them separately.

For $x \in \Omega$, by Lemma 3.3 and equation (5), we have

$$\int_{\overline{\overline{\Omega}}} \widetilde{\Psi}_\epsilon(p, x; x-y) y^\alpha dy = x^\alpha, \quad \alpha = 0, 1, \ldots, p+1. \tag{34}$$

So we can write

$$\begin{aligned} u(x) - u_\epsilon(x) =& Q_j^{p+1}u(x) - \int_{\overline{\overline{\Omega}}} \widetilde{\Psi}_\epsilon(p, x; x-y) Q_j^{p+1}u(y)dy \\ &+ R_j^{p+1}u(x) - \int_{\overline{\overline{\Omega}}} \widetilde{\Psi}_\epsilon(p, x; x-y) R_j^{p+1}u(y)dy, \end{aligned}$$

where $Q_j^{p+1}u$ is the Taylor polynomial of degree $p+1$ of u averaged over B_j, and $R_j^{p+1}u$ is the remainder. By equation (34), we have

$$Q_j^{p+1}u(x) = \int_{\overline{\overline{\Omega}}} \widetilde{\Psi}_\epsilon(p, x; x-y) Q_j^{p+1}u(y)dy, \quad x \in \Omega\,.$$

So one can follow the previous arguments to show that

$$\|u - u_\epsilon\|_{W^{l,q}(B_j \cap \Omega)} \leq C\epsilon^{p+2-l}\|u\|_{W^{p+2,q}(\hat{B}_j \cap \Omega)}\,,$$

for $l = 0, 1, \cdots, p+2$. Now combine with fact that

$$\|u - u_\epsilon\|_{W^{l,q}(B_j \cap \Omega_{bl})} \leq C\epsilon^{p+1-l}\|u\|_{W^{p+1,q}(\hat{B}_j \cap \Omega_{bl})}\,,$$

for $l = 0, 1, \cdots, p+1$, we have finally

$$\begin{aligned}
\|u(x) - u_\epsilon(x)\|_{W^{l,q}(\overline{\overline{\Omega}})} &\leq \sum_{j: B_j \cap \Omega \neq \emptyset} \|u - u_\epsilon\|_{W^{l,q}(\hat{B}_j \cap \Omega)} + \sum_{j: B_j \cap \Omega_{bl} \neq \emptyset} \|u - u_\epsilon\|_{W^{l,q}(B_j \cap \Omega)}\,, \\
&\leq C\epsilon^{p+2-l}\|u\|_{W^{p+2,q}(\Omega)} + C\epsilon^{p+1-l}\|u\|_{W^{p+1,q}(\Omega_{bl})}\,, \\
&\leq C\epsilon^{p+2-l}\|u\|_{W^{p+2,q}(\Omega)} + C\epsilon^{p+1+1/q-l}\|u\|_{W^{p+1,q}(\overline{\overline{\Omega}})}\,, \\
&\leq C\epsilon^{p+1+1/q-l}\|u\|_{W^{p+2,q}(\overline{\overline{\Omega}})}\,.
\end{aligned}$$

□

4. Discrete RK approximation error estimates for selected RK support sizes

In this section we investigate super-convergence for the discrete RK approximation. Continuous RK approximation discussed in section 3 has little use in practice, though it gives us some insights on how to obtain super-convergence in discrete RK approximation. From the previous section we have established a clear understanding of the origin of super-convergence. Intuitively, we can hope for super-convergence to happen with even order discrete RK approximation if the discrete moment m_α vanishes for α being an odd number. However, this condition is hard to satisfy if particles are not uniformly distributed. Therefore in this section, we only consider the uniform discretization of the domain $\overline{\overline{\Omega}}$. We assume that $\{x_k\}_{k=1}^I$ is the uniformly distributed with $h = x_k - x_{k-1}$ to be the spacing. By construction, the p-th order discrete RK approximation also satisfies p-th order reproducing condition, so similar to the continuous case, the L^2 approximation

error is at least $O(\epsilon^{p+1})$ for the p-th order discrete RK approximation. We will not repeat the arguments here since they are almost identical to the continuous case. The super-convergence, however, is different.

Unlike continuous moment, if α is odd, the discrete moment $m_\alpha(x)$ is not always zero for $x \in \Omega$. However, we will show in the following that this can be made true with carefully selected window functions and RK support sizes. To achieve this, we need to utilize the Strang-Fix condition ([6]) to characterize the kernel functions. We recall that a function $f(x)$ is said to satisfy the k-th order Strang-Fix condition, if the following two conditions are satisfied:

$$\widehat{f}(0) = 1, \text{ and} \tag{35}$$

$$D_\xi^\alpha \widehat{f}(\xi)\Big|_{2\pi j} = 0, \quad \forall j \in \mathbb{Z}\backslash\{0\},\ \alpha \le k\,. \tag{36}$$

Here $\widehat{f}(\xi)$ is the Fourier transform of $f(x)$ defined as

$$\widehat{f}(\xi) = \int_{-\infty}^{\infty} f(x) e^{-i\xi x} dx\,,$$

and $D_\xi^\alpha \widehat{f}$ is the α-th derivative of $\widehat{f}$. Since for us the scaling factor can always be absorbed into the correction function, the condition (35) can actually be dropped because it is a normalization of the function f. In addition, we will use a more generalized version of condition (36):

$$D_\xi^\alpha \widehat{f}(\xi)\Big|_{\frac{2\pi j}{h}} = 0, \quad \forall j \in \mathbb{Z}\backslash\{0\}\,,$$

where h is the mesh spacing. So following the notation in [17], we define a special class of functions that satisfies the generalized k-th order Strang-Fix condition as

$$\mathcal{SF}_h^{(k)} = \{f : D_\xi^\alpha \widehat{f}(\xi)\Big|_{\frac{2\pi j}{h}} = 0, \quad \forall j \in \mathbb{Z}\backslash\{0\},\ 0 \le \alpha \le k\} \tag{37}$$

It turns out that the discrete moment $m_\alpha(x)$ for x in the interior of the domain has an equivalent form as in the following lemma.

Lemma 4.1. *Assume that the kernel function $\phi_\epsilon \in \mathcal{SF}_h^{(k)}$, then the discrete moment $m_\alpha(x)$ defined by (17) does not depend on x in the interior of*

domain and is given by

$$m_\alpha(x) = \frac{1}{h}\int_{\mathbb{R}} z^\alpha \phi_\epsilon(z)dz\,, \tag{38}$$

for $\alpha \le k$ *and* $x \in \Omega$.

Proof. First we recall Poisson's summation formula (see e.g. [2]):

$$\sum_{j\in\mathbb{Z}} f(x+jh) = \frac{1}{h}\sum_{j\in\mathbb{Z}} \widehat{f}\left(2\pi\frac{j}{h}\right) e^{i2\pi x\frac{j}{h}}\,.$$

Assume that $x_k = kh$ without loss of generality. For $x \in \Omega$, the discrete moment can be written as

$$\begin{aligned} m_\alpha(x) &= \sum_{j=1}^{I}(x-x_j)^\alpha\phi_\epsilon(x-x_j) = \sum_{j\in\mathbb{Z}}(x+jh)^\alpha\phi_\epsilon(x+jh), \\ &= \frac{i^\alpha}{h}\sum_{j\in\mathbb{Z}} D_\xi^\alpha\widehat{\phi_\epsilon}\left(2\pi\frac{j}{h}\right)e^{i2\pi x\frac{j}{h}}, \\ &= \frac{i^\alpha}{h}D_\xi^\alpha\widehat{\phi_\epsilon}(0), \end{aligned} \tag{39}$$

where we used Poisson's summation formula and the generalized Strang-Fix condition for ϕ_ϵ. Now since

$$D_\xi^\alpha\widehat{\phi_\epsilon}(\xi) = \int_{\mathbb{R}}(-ix)^\alpha\phi_\epsilon(x)e^{-i\xi x}dx\,,$$

we then have

$$\frac{i^\alpha}{h}D_\xi^\alpha\widehat{\phi_\epsilon}(0) = \frac{1}{h}\int_{\mathbb{R}} x^\alpha\phi_\epsilon(x)dx\,.$$

□

From equation (38), it is easily seen that the discrete moment $m_\alpha(x)$ vanishes for $x \in \Omega$ if α is an odd number, by the fact that ϕ_ϵ is a symmetric kernel. Then it is straightforward to go through the same process from Lemma 3.1 to Lemma 3.3. Here we only present a discrete version of Lemma 3.3. For convenience we denote $\Psi_k(p,x)(k=1,\cdots,I)$ to be the RK shape function of p-th order.

Lemma 4.2. *Assume that the kernel function* $\phi_\epsilon \in \mathcal{SF}_h^{(2p_0+1)}$*, where* p_0 *is some nonnegative integer, then for all* $p \le p_0$ *and* p *being an even number,*

the RK shape functions of p-th and $(p+1)$-th order are identical in the interior of the domain, namely

$$\Psi_k(p,x) = \Psi_k(p+1,x), \quad x \in \Omega,\ p \le p_0,\ p \text{ is even}.$$

Proof. This is a result of Lemma 4.1. The proof is essentially the same as the arguments in Lemma 3.2 and Lemma 3.3. □

Finally, we assume that the particle distribution is always (ϵ, p)-regular, a notion introduced by [5], so that all the analytical tools in [5] can be used. the theorem for discrete RK approximation error estimates is the following.

Theorem 4.3. *Assume that the window function $\phi \in C^{p+2}$, and $u \in W^{p+2,q}(\overline{\overline{\Omega}})$ is proper. Suppose $\phi_\epsilon \in \mathcal{SF}_h^{(2p+1)}$, the error estimate for the discrete RK approximation is as follows:*
if p is odd,

$$\|u - u^I\|_{W^{l,q}(\overline{\overline{\Omega}})} \le C\epsilon^{p+1-l}\|u\|_{W^{p+1,q}(\overline{\overline{\Omega}})},$$

and if p is even,

$$\|u - u^I\|_{W^{l,q}(\overline{\overline{\Omega}})} \le C\epsilon^{p+1+1/q-l}\|u\|_{W^{p+2,q}(\overline{\overline{\Omega}})},$$

for $l = 0, 1, \cdots, p+1$.

Proof. The proof is a discrete adaptation to the previous continuous result, which can also be obtained following the analysis of [5]. The super-convergence for p being even is realized by the application of Lemma 4.2. □

4.1. B-spline functions as window functions

Theorem 4.3 tells us that in general, we expect the discrete RK approximation of even order to have super-convergence if we select the sufficiently smooth window function such that $\phi_\epsilon \in \mathcal{SF}_h^{(2p+1)}$. In practice, the window function $\phi(x)$ is usually chosen as B-spline functions. The following lemma reveals the good properties of B-spline functions that allow us to have super-convergence.

Lemma 4.4. *Assume that the window function ϕ is supported on $[-1,1]$ and it is the B-spline of degree $n \ge 2p+1$. Assume also that the RK support size is chosen to be $\epsilon = \frac{n+1}{2} r_0 h$, for r_0 being a positive integer, then $\phi_\epsilon \in \mathcal{SF}_h^{(2p+1)}$, and thus the convergence results in Theorem 4.3 are achieved.*

Proof. We introduce a rectangular function

$$\beta^0(x) = \begin{cases} 1, & x \in [-\frac{1}{2}, \frac{1}{2}], \\ 0, & \text{otherwise}, \end{cases}$$

and its Fourier transform is given by

$$\widehat{\beta^0}(\xi) = \frac{\sin(\xi/2)}{\xi/2}.$$

B-spline function of degree n, can be written as the convolution of $n+1$ rectangular functions ([16]),

$$\beta^n(x) = \beta^0 * \beta^0 * \cdots * \beta^0(x),$$

and thus

$$\widehat{\beta^n}(\xi) = \left[\frac{\sin(\xi/2)}{\xi/2}\right]^{n+1}.$$

Here we normalize the support of the B-spline to $[-1, 1]$ to get our window function

$$\phi(x) = \beta^n\left(\frac{n+1}{2}x\right). \tag{40}$$

So

$$\phi_\epsilon(x) = \frac{1}{\epsilon}\phi\left(\frac{x}{\epsilon}\right) = \frac{1}{\epsilon}\beta^n\left(\frac{x}{r_0 h}\right),$$

where we used $\epsilon = \frac{n+1}{2} r_0 h$. Thus we have

$$\widehat{\phi_\epsilon}(\xi) = \frac{r_0 h}{\epsilon}\widehat{\beta^n}\left(r_0 h \xi\right) = \frac{r_0 h}{\epsilon}\left[\frac{\sin(r_0 h \xi/2)}{r_0 h \xi/2}\right]^{n+1}. \tag{41}$$

The derivatives of $\widehat{\phi_\epsilon}$ are given by

$$D_\xi^\alpha \widehat{\phi_\epsilon}(\xi) = \frac{r_0 h}{\epsilon}\sum_{k=0}^{\alpha}\binom{\alpha}{k} D_\xi^{\alpha-k}(\sin\left(r_0 h\xi/2\right))^{n+1} D_\xi^k\left(\left(\frac{1}{r_0 h \xi/2}\right)^{n+1}\right),$$

Now that

$$\sin\left(r_0 h \xi/2\right)\Big|_{\xi=\frac{2\pi j}{h}} = 0, \quad j \in \mathbb{Z},$$

and if $\alpha \leq n$, $\sin(r_0 h\xi/2)$ is in every term of $D_\xi^\alpha \widehat{\phi}_\epsilon(\xi)$, we have

$$D_\xi^\alpha \widehat{\phi}_\epsilon(\xi)\Big|_{\xi=2\pi j} = 0, \quad j \in \mathbb{Z}\backslash\{0\},$$

which proves that $\phi_\epsilon \in \mathcal{SF}_h^{(2p+1)}$. □

Lemma 4.4 shows that the popular choices of B-spline functions as window functions can achieve the assumptions made in Theorem 4.3. Therefore, lemma 4.4 can be used as guidelines on how to select window function and RK support in order to achieve super-convergence. We will see in Section 6 that numerical experiments verify our theorem.

5. Multi-dimensional RK Approximation

We work with one-dimensional problems previously for better representation of the work. Our method can actually be easily generalized to the analysis of multi-dimensional RK approximation. Let $d > 1$, we consider an open bounded domain $\overline{\overline{\Omega}} \subset \mathbb{R}^d$. The boundary layer of $\overline{\overline{\Omega}}$ is given by

$$\Omega_{bl} = \{\boldsymbol{x} \in \overline{\overline{\Omega}} : \text{dist}(x, \partial\Omega) < \epsilon\}.$$

The interior of $\overline{\overline{\Omega}}$ is then the complement of Ω_{bl} in $\overline{\overline{\Omega}}$. A point in $\mathbb{R}^d$ is denoted by $\boldsymbol{x} = (x_1, \ldots, x_d)^T$. A multi-index is a collection of d nonnegative integers, $\boldsymbol{\alpha} = (\alpha_1, \ldots, \alpha_d)$ and its length is expressed as $|\boldsymbol{\alpha}| = \sum_{i=1}^d \alpha_i$. For a given $\boldsymbol{\alpha}$, we write $\boldsymbol{x}^{\boldsymbol{\alpha}} = x_1^{\alpha_1} \ldots x_d^{\alpha_d}$.

Now instead of (3), the kernel function $\phi_\epsilon(\boldsymbol{x})$ in multi-dimension is defined as

$$\phi_\epsilon(\boldsymbol{x}) = \frac{1}{\epsilon^d}\phi\left(\frac{|\boldsymbol{x}|}{\epsilon}\right), \quad \boldsymbol{x} \in \mathbb{R}^d. \tag{42}$$

The row vector $\boldsymbol{H}_p^T(\boldsymbol{x}-\boldsymbol{y})$ consists of multivariate monomial basis functions of degree p arranged in certain lexicographical order:

$$\boldsymbol{H}_p^T(\boldsymbol{x}-\boldsymbol{y}) = [(\boldsymbol{x}-\boldsymbol{y})^{\boldsymbol{\alpha}}]_{|\boldsymbol{\alpha}|\leq p} \in \mathbb{R}^{N_p},$$

where N_p is the dimension of the polynomial space of degree p and is defined as

$$N_p = \binom{p+d}{d}.$$

The continuous moment matrix $\widetilde{\boldsymbol{M}}_p(\boldsymbol{x}) \in \mathbb{R}^{N_p \times N_p}$ is given by

$$\widetilde{\boldsymbol{M}}_p(\boldsymbol{x}) = \int_{\overline{\Omega}} \boldsymbol{H}_p(\boldsymbol{x}-\boldsymbol{y})\phi_\epsilon(\boldsymbol{x}-\boldsymbol{y})\boldsymbol{H}_p^T(\boldsymbol{x}-\boldsymbol{y})d\boldsymbol{y},$$

and each entry of $\widetilde{\boldsymbol{M}}_p(\boldsymbol{x})$ is written as

$$\widetilde{m}_{\boldsymbol{\alpha}}(\boldsymbol{x}) = \int_{\overline{\Omega}} (\boldsymbol{x}-\boldsymbol{y})^{\boldsymbol{\alpha}}\phi_\epsilon(\boldsymbol{x}-\boldsymbol{y})d\boldsymbol{y}, \quad |\boldsymbol{\alpha}| \le 2p\,. \tag{43}$$

Therefore, we arrive at the continuous approximation in multi-dimension as

$$u_{\boldsymbol{\epsilon}}(\boldsymbol{x}) = \int_{\overline{\Omega}} \widetilde{\Psi}_\epsilon(\boldsymbol{x};\boldsymbol{x}-\boldsymbol{y})u(\boldsymbol{y})d\boldsymbol{y}\,,$$

where

$$\widetilde{\Psi}_\epsilon(\boldsymbol{x};\boldsymbol{x}-\boldsymbol{y}) = \boldsymbol{H}_p^T(\boldsymbol{x}-\boldsymbol{y})\widetilde{\boldsymbol{M}}_p^{-1}(\boldsymbol{x})\boldsymbol{H}_p(\boldsymbol{0})\phi_\epsilon(\boldsymbol{x}-\boldsymbol{y})\,.$$

With the continuous multi-dimensional RK approximation defined, it is straightforward to define the corresponding discrete RK approximation following the work in 1d, which we will omit here.

Now by the definition of the moment $\widetilde{m}_{\boldsymbol{\alpha}}(\boldsymbol{x})$ in equation (43), we observe that it is zero for $\boldsymbol{x}$ in the interior of the domain if any one of components of $\boldsymbol{\alpha}$ is an odd number, which is a multi-dimensional generalization of Lemma 3.1. We first define some notations for convenience of presentation. We define the set $\mathcal{I} = \{\boldsymbol{\alpha} = (\alpha_1, \alpha_2, \cdots, \alpha_d) \in \mathbb{N}^d : |\boldsymbol{\alpha}| \le p\}$, and define two subsets of $\mathcal{I}$ as

$$\begin{aligned}
&\mathcal{E} = \{\boldsymbol{\alpha} \in \mathcal{I} : \alpha_i \text{ are even numbers for all } 1 \le i \le d\}, \text{ and}\\
&\mathcal{O} = \mathcal{I}\backslash\mathcal{E}\,.
\end{aligned}$$

Notice that $\mathcal{O}$ is the set of all indices $\boldsymbol{\alpha}$ with at least one component to be an odd number. Now the multi-dimensional version of Lemma 3.1 is the following.

Lemma 5.1. *For $\boldsymbol{x} \in \Omega$, the moment $\widetilde{m}_{\boldsymbol{\alpha}}(\boldsymbol{x}) = 0$ if $\boldsymbol{\alpha} \in \mathcal{O}$.*

Proof. For $\boldsymbol{x}$ in the interior of the domain, the moment given by (43) is actually

$$\widetilde{m}_{\boldsymbol{\alpha}}(\boldsymbol{x}) = \int_{\mathbb{R}^d} \boldsymbol{z}^{\boldsymbol{\alpha}}\phi_\epsilon(\boldsymbol{z})d\boldsymbol{z}\,. \tag{44}$$

Since ϕ_ϵ is a radially symmetric function, it is obvious that if one of the components of α is an odd number, then the integral given by (44) is zero.

□

We now give a multi-dimensional version of Lemma 3.2.

Lemma 5.2. *Let* $\boldsymbol{b}_p(\boldsymbol{x}) = \widetilde{\boldsymbol{M}}_p^{-1}(\boldsymbol{x})\boldsymbol{H}_p(\boldsymbol{0})$ *and let* $b_p^{(\boldsymbol{\alpha})}(|\boldsymbol{\alpha}| \le p)$ *be the components of* $\boldsymbol{b}_p$*. For* $\boldsymbol{x} \in \Omega$*, we have*

(a) $b_p^{(\boldsymbol{\alpha})}(\boldsymbol{x}) = 0$ *if* $\boldsymbol{\alpha} \in \mathcal{O}$*, and*

(b) $b_p^{(\boldsymbol{\alpha})}(\boldsymbol{x}) = b_{p+1}^{(\boldsymbol{\alpha})}(\boldsymbol{x})$ *for* $p = 2k$*, where* $k \in \mathbb{N}$*.*

Proof. The basic idea of proof is again by splitting the system $\widetilde{\boldsymbol{M}}_p(\boldsymbol{x})\boldsymbol{b}_p(\boldsymbol{x}) = \boldsymbol{H}_p(\boldsymbol{0})$ into two linear systems. Notice that in 1d, the linear systems (27) and (30) are decomposed into two smaller systems. The common feature is that after the decomposition, the smaller systems (28) and (31) contain only the components of $\boldsymbol{b}_p$ with even upper indices. Here such decomposition for multi-dimensional problem follows similarly.

Now we split the vector $\boldsymbol{b}_p(\boldsymbol{x})$ into two sub-vectors by defining

$$\boldsymbol{b}_p^{even}(\boldsymbol{x}) = [\boldsymbol{b}_p^{(\boldsymbol{\alpha})}(\boldsymbol{x})]_{\boldsymbol{\alpha}\in\mathcal{E}}, \text{ and } \boldsymbol{b}_p^{odd}(\boldsymbol{x}) = [\boldsymbol{b}_p^{(\boldsymbol{\alpha})}(\boldsymbol{x})]_{\boldsymbol{\alpha}\in\mathcal{O}}\,.$$

We then define sub-matrices of $\widetilde{\boldsymbol{M}}_p(\boldsymbol{x})$ as

$$\begin{aligned}\widetilde{\boldsymbol{M}}_p^{even}(\boldsymbol{x}) &= (\widetilde{m}_{\boldsymbol{\alpha}+\boldsymbol{\beta}}(\boldsymbol{x}))_{\boldsymbol{\alpha}\in\mathcal{E},\boldsymbol{\beta}\in\mathcal{E}}\,, \text{ and}\\ \widetilde{\boldsymbol{M}}_p^{odd}(\boldsymbol{x}) &= (\widetilde{m}_{\boldsymbol{\alpha}+\boldsymbol{\beta}}(\boldsymbol{x}))_{\boldsymbol{\alpha}\in\mathcal{O},\boldsymbol{\beta}\in\mathcal{O}}\,.\end{aligned}$$

It is obvious that $\widetilde{\boldsymbol{M}}_p^{even}(\boldsymbol{x})$ and $\widetilde{\boldsymbol{M}}_p^{odd}(\boldsymbol{x})$ are both invertible if the original matrix $\widetilde{\boldsymbol{M}}_p(\boldsymbol{x})$ is invertible. Notice that the other two sub-matrices of $\widetilde{\boldsymbol{M}}_p(\boldsymbol{x})$ given by $(\widetilde{m}_{\boldsymbol{\alpha}+\boldsymbol{\beta}}(\boldsymbol{x}))_{\boldsymbol{\alpha}\in\mathcal{E},\boldsymbol{\beta}\in\mathcal{O}}$ and $(\widetilde{m}_{\boldsymbol{\alpha}+\boldsymbol{\beta}}(\boldsymbol{x}))_{\boldsymbol{\alpha}\in\mathcal{O},\boldsymbol{\beta}\in\mathcal{E}}$ are in fact zero since by Lemma 5.2 the moment $\widetilde{m}_{\boldsymbol{\gamma}}(\boldsymbol{x})$ is zero if $\boldsymbol{\gamma} \in \mathcal{O}$. We can then rearrange the rows and columns in the system $\widetilde{\boldsymbol{M}}_p(\boldsymbol{x})\boldsymbol{b}_p(\boldsymbol{x}) = \boldsymbol{H}_p(\boldsymbol{0})$ such that it is given by the following block matrices

$$\begin{bmatrix}\widetilde{\boldsymbol{M}}_p^{even}(\boldsymbol{x}) & \boldsymbol{0}\\ \boldsymbol{0} & \widetilde{\boldsymbol{M}}_p^{odd}(\boldsymbol{x})\end{bmatrix}\begin{bmatrix}\boldsymbol{b}_p^{even}(\boldsymbol{x})\\ \boldsymbol{b}_p^{odd}(\boldsymbol{x})\end{bmatrix} = \begin{bmatrix}\boldsymbol{e}_1\\ \boldsymbol{0}\end{bmatrix}, \tag{45}$$

where $\boldsymbol{e}_1 = [1, 0, \cdots, 0]^T$. Naturally, (45) splits into two linear systems

$$\widetilde{\boldsymbol{M}}_p^{even}(\boldsymbol{x})\boldsymbol{b}_p^{even}(\boldsymbol{x}) = \boldsymbol{e}_1\,, \text{ and} \tag{46}$$

$$\widetilde{\boldsymbol{M}}_p^{odd}(\boldsymbol{x})\boldsymbol{b}_p^{odd}(\boldsymbol{x}) = \boldsymbol{0}\,. \tag{47}$$

Equation (47) implies that $\boldsymbol{b}_p^{odd}(\boldsymbol{x}) = \mathbf{0}$, which is exactly (a). Moreover, (b) is not hard to seen by looking at equation (46) for $p = 2k$ and $p = 2k+1$. □

As soon as one has the multi-dimensional version of Lemma 3.2, it is clear that there is no obstacle in obtaining the convergence theorem in multi-dimension. We believe that the proof is similar enough to the 1d case so that it is omitted here. For completeness, we give the final theorem for the multi-dimensional continuous RK approximation is given as follows.

Theorem 5.3. *Assume that the window function $\phi \in C^{p+2}$, and $u \in W^{p+2,q}(\overline{\overline{\Omega}})$ is proper. Then the error estimate for the d-dimensional continuous RK approximation is as follows:*
if p is odd,

$$\|u - u_\epsilon\|_{W^{l,q}(\overline{\overline{\Omega}})} \leq C\epsilon^{p+1-l}\|u\|_{W^{p+1,q}(\overline{\overline{\Omega}})},$$

and if p is even,

$$\|u - u_\epsilon\|_{W^{l,q}(\overline{\overline{\Omega}})} \leq C\epsilon^{p+1+d/q-l}\|u\|_{W^{p+2,q}(\overline{\overline{\Omega}})},$$

for $l = 0, 1, \cdots p+1$.

For the discrete RK approximation, we need to modify the definition of the set of functions with Strang-Fix property. Instead of (37), we now define

$$\mathcal{SF}_h^{(k)} = \{f : D_{\boldsymbol{\xi}}^{\boldsymbol{\alpha}} \widehat{f}(\boldsymbol{\xi})\Big|_{\frac{2\pi \boldsymbol{j}}{h}} = 0, \quad \forall\, j \in \mathbb{Z}^d \backslash \{0\},\, 0 \leq \alpha \leq k\}, \tag{48}$$

where $D_{\boldsymbol{\xi}}^{\boldsymbol{\alpha}} = D_{\xi_1}^{\alpha_1} D_{\xi_2}^{\alpha_2} \cdots D_{\xi_d}^{\alpha_d}$. Then the multi-dimensional version of Theorem 4.3 is given as follows.

Theorem 5.4. *Assume that the window function $\phi \in C^{p+2}$, and $u \in W^{p+2,q}(\overline{\overline{\Omega}})$ is proper. Suppose $\phi_\epsilon \in \mathcal{SF}_h^{(2p+1)}$, then the error estimate for the d-dimensional discrete RK approximation is as follows:*
if p is odd,

$$\|u - u^I\|_{W^{l,q}(\overline{\overline{\Omega}})} \leq C\epsilon^{p+1-l}\|u\|_{W^{p+1,q}(\overline{\overline{\Omega}})},$$

and if p is even,

$$\|u - u^I\|_{W^{l,q}(\overline{\overline{\Omega}})} \leq C\epsilon^{p+1+d/q-l}\|u\|_{W^{p+2,q}(\overline{\overline{\Omega}})},$$

for $l = 0, 1, \cdots p+1$.

6. Numerical experiments

Cubic B-spline is widely used as the window function in RK approximations, because it guarantees that $u^I \in C^2(\overline{\overline{\Omega}})$. In this section, $\phi(x)$ is defined by equation (40) with $n = 3$. By Lemma 4.4 and Theorem 4.3, we have super-convergence of the RK approximation of constant basis ($p = 0$) if the RK support $\epsilon = \frac{n+1}{2} r_0 h = 2r_0 h$, where $r_0 \in \mathbb{N}$. We are going to verify Theorem 4.3 with $l = 0$ and $q = 2$, namely we will look at the L^2 error between a function and its discrete RK approximation with the expectation of half-order super-convergence for the case $p = 0$.

Figure 2 shows the pointwise error of using constant RK basis ($p = 0$) to approximate linear function the $u(x) = x$ on the domain $\overline{\overline{\Omega}} = (0, 1)$. In Figure 2, 11 particles are positioned uniformly and RK support $\epsilon = 2h$ ($r_0 = 1$). We see that the approximation error is zero everywhere in the interior of the domain. This is to say the RK approximation with constant basis reproduces exactly linear functions in the interior of the domain. In general, the RK shape function of constant basis satisfies first order reproducing condition for points in the interior of the domain with support size $\epsilon = 2r_0 h$, where r_0 is a positive integer.

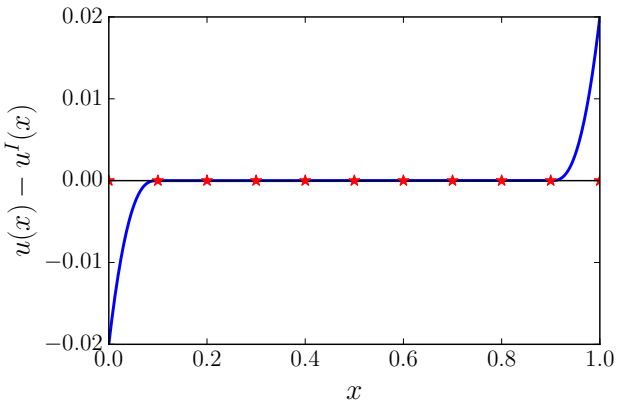

Figure 2: Error distribution of approximating a linear function $u(x) = x$ using constant RK basis with $h = 0.1$ and $\epsilon = 2h$. Cubic B-spline is the window function.

Convergence studies of approximating $u(x) = e^x$ are shown in Figure 3, 4 and 5. In Figure 3, constant RK basis ($p = 0$) is used with RK support $\epsilon = 2h$. The L^2 convergence rate on Ω is observed to be second order and the L^2 convergence rate over the whole domain $\overline{\overline{\Omega}}$ is observed to be $O(h^{1.5})$, which agrees with our theorem. Figure 3 can be compared with Figure 4,

where linear RK basis ($p = 1$) is used with RK support $\epsilon = 2h$. The L^2 convergence rates are second order on both Ω and $\overline{\overline{\Omega}}$. Similar behaviors are observed for all support size $\epsilon = 2r_0 h$, where r_0 is a positive integer. More generally, to see the super-convergence of RK approximation for $p \geq 2$, higher order B-spline functions need to be used, using the guidelines given by Lemma 4.2. In Figure 5, quadratic RK basis ($p = 2$) is employed with RK support $\epsilon = 3h$ and the window function is the fifth-order B-spline. The L^2, H^1 and H^2 convergence rates on Ω are 4.0, 3.0 and 2.0 respectively and they are 3.5, 2.5 and 1.5 on $\overline{\overline{\Omega}}$. We observe super-convergence for constant and quadratic RK basis and our numerical experiments verify the results of Lemma 4.2.

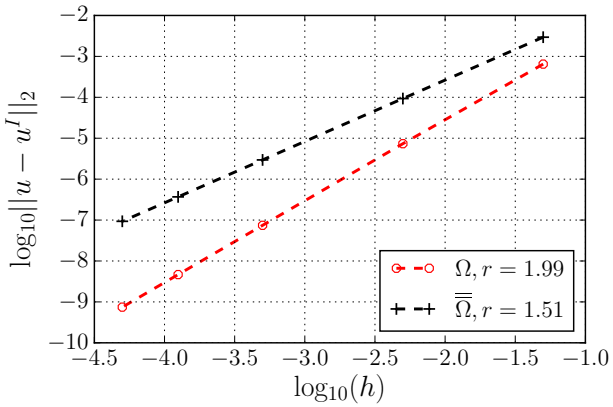

Figure 3: Convergence study of approximating $u(x) = e^x$ using constant RK basis with $\epsilon = 2h$. r is the rate of convergence and cubic B-spline is the window function.

7. The discussion on general RK support sizes

The analysis in section 4 does not hold for general RK support sizes except for these discussed in lemma 4.4 because $\phi_\epsilon \notin \mathcal{SF}_h^{(2p+1)}$ for arbitrary ϵ. Thus one do not expect super-convergence of RK approximation with arbitrary RK support size. We present the error estimates of RK approximation with arbitrary RK support sizes which can be found in [5, 10] as follows:

$$\|u - u^I\|_{W^{l,q}(\overline{\overline{\Omega}})} \leq C\epsilon^{p+1-l}\|u\|_{W^{p+1,q}(\overline{\overline{\Omega}})}, \quad \text{for } l = 0, 1, \cdots, p+1. \tag{49}$$

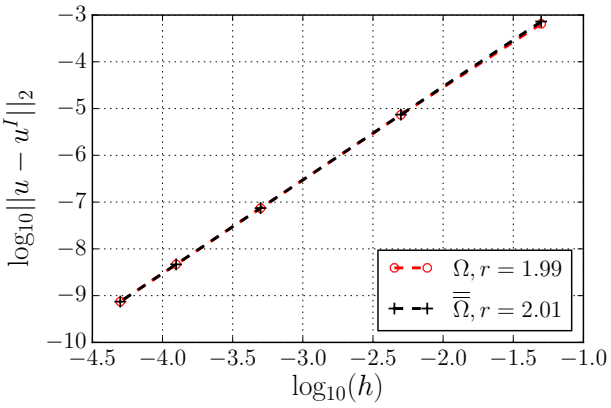

Figure 4: Convergence study of approximating $u(x) = e^x$ using linear RK basis with $\epsilon = 2h$. r is the rate of convergence and cubic B-spline is the window function.

In Section 4, we showed that in general if B-spline of order n is the window function, then we have super-convergence for even order RK basis with support size $\epsilon = \frac{n+1}{2} r_0 h$. In general, for an arbitrary RK support size, we do not expect such super-convergence. Figure 6 shows the error distribution of using constant RK basis to approximate linear function the $u(x) = x$, but with a support size $\epsilon = h$. We do not see the exact reproduce of linear function in the interior of the domain, in comparison with Figure 2 using the support size $\epsilon = 2h$. However, we do observe that the error vanishes the at grid points ($x = x_i$) and midpoints between grid points ($x = (x_i + x_{i+1})/2$). This is a general fact for all support sizes because the grids are symmetrically distributed centered at these special points $x = x_i$ and $x = (x_i + x_{i+1})/2$, which makes the odd order discrete moments at these points to be zero, and we can easily derive a higher order reproducing relation at those special points for even order RK basis.

In practice, however, one often observes super-convergence in L^2 norm for even order RK basis with a support size ϵ not exactly equal to $\frac{n+1}{2} r_0 h$ ([10, 14]). These observations do not contradict equation (49) and we call this phenomenon the *pseudo-super-convergence*.

Remark 7.1. *Pseudo-super-convergence is the phenomenon that some numerical examples do not exhibit the real super-convergence phenomena but are due to insufficient refinement of h.*

First, at a generic point x ($x \neq x_i$ and $x \neq (x_i + x_{i+1})/2$) in the interior of the domain, although the odd order discrete moments do not vanish com-

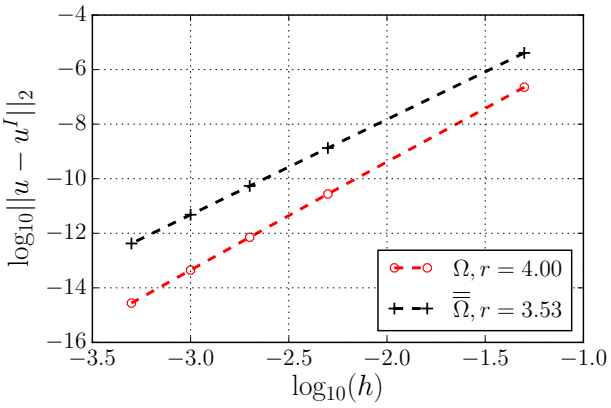

(a) L^2 norm

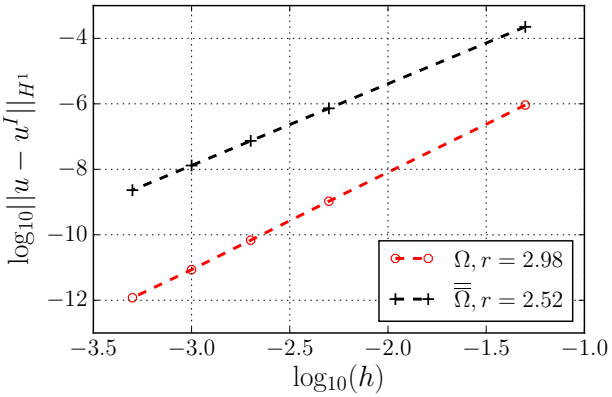

(b) H^1 norm

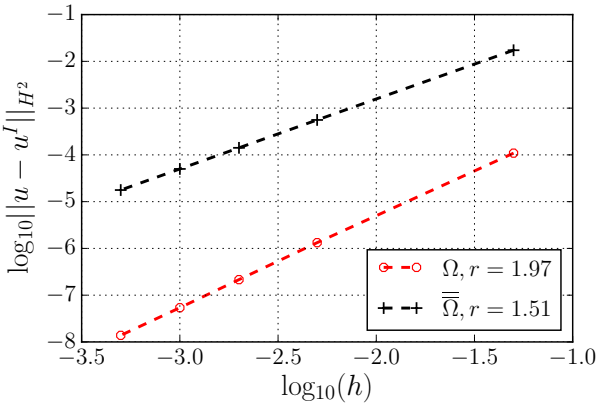

(c) H^2 norm

Figure 5: Convergence study of approximating $u(x) = e^x$ using linear RK basis with $\epsilon = 3h$. r is the rate of convergence and fifth-order B-spline is the window function.

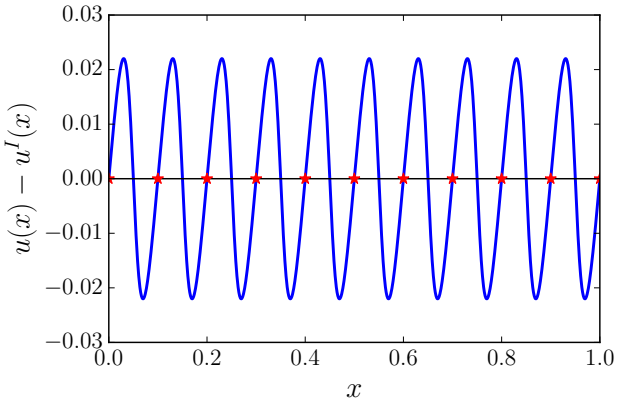

Figure 6: Error distribution of approximating a linear function $u(x) = x$ using constant RK basis with $h = 0.2$ and $\epsilon = h$. Cubic B-spline is the window function.

pletely, but they are diminishing as the ratio ϵ/h grows, since more sampling points are used to calculate the numerical integral of anti-symmetric functions. We see clearly in Figure 7 that with the increase of the ratio ϵ/h, the errors in the interior of the domain relative to the boundary are diminishing for the case of approximating linear functions by the constant RK approximation. Thus in the region where h is not refined enough, the dominant error comes from the boundary and thus we observe super-convergence for p being even. However, for a fixed ratio ϵ/h, the approximation error on Ω will eventually play the significant role with the refinement of h. Thus convergence rate drops back to $p+1$ in the region where h is smaller than some threshold. The differentiation of two regions is typical in a RK approximation with pseudo-super-convergence.

Figure 8 studies pseudo-super-convergence phenomena. We approximate $u(x) = e^x$ by RK with constant basis using cubic B-spline as the window function. Figure 8 shows the clear transition between two different regions of convergence rates. In Figure 8a, the support size $\epsilon = 1.7h$ is used. When $h > 1E-2.5$, the major approximation error comes from the boundary, thus we see a convergence rate of $r = 1.5$. When $h < 1E-2.5$, the error on Ω starts to play the dominant role. The convergence rate over the whole domain gradually changes from $r = 1.5$ to $r = 1.0$. We observe similar pattern of such transition in Figure 8b where $\epsilon = 2.7h$. The difference is that with a larger ratio ϵ/h, the transition of error contribution comes at a smaller mesh size where $h \approx 1E-4.5$. The transition point moves further when we keep increasing the ratio ϵ/h. If one further increases the ratio

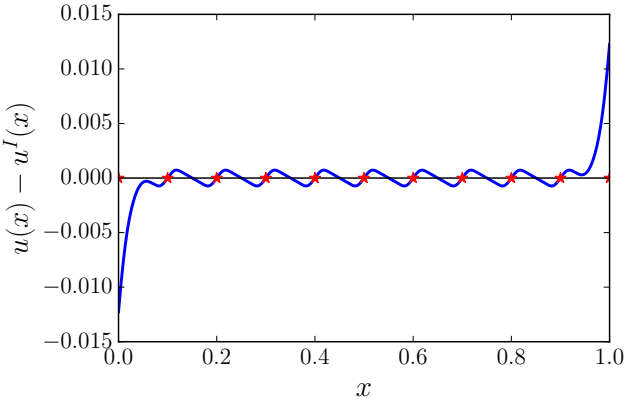

(a) $h = 0.1, \epsilon = 1.7h$

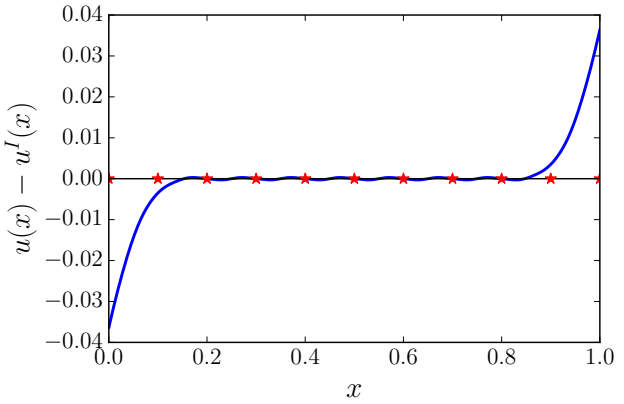

(b) $h = 0.1, \epsilon = 2.7h$

Figure 7: Error distribution of approximating a linear function $u(x) = x$ using constant RK basis with support sizes $\epsilon = 1.7h$ and $\epsilon = 2.7h$. Cubic B-spline is the window function.

ϵ/h, then the transition happens at even smaller h. When the ratio ϵ/h is large enough such that the transition point is around machine precision, i.e., Figure 9, one always observes super-convergence in numerical experiments. However, such super-convergence is not a mathematical property but just a numerical artifact, and thus it bears the name pseudo-super-convergence.

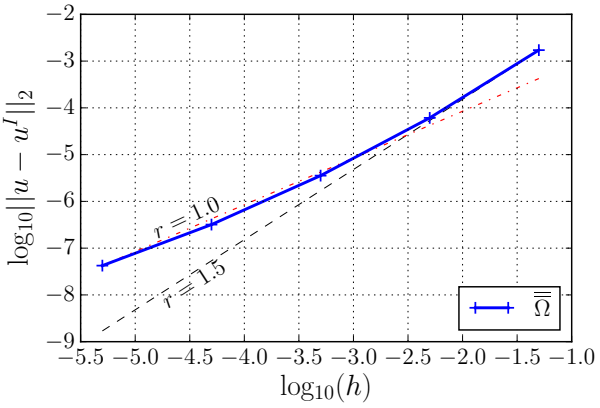

(a) $\epsilon = 1.7h$

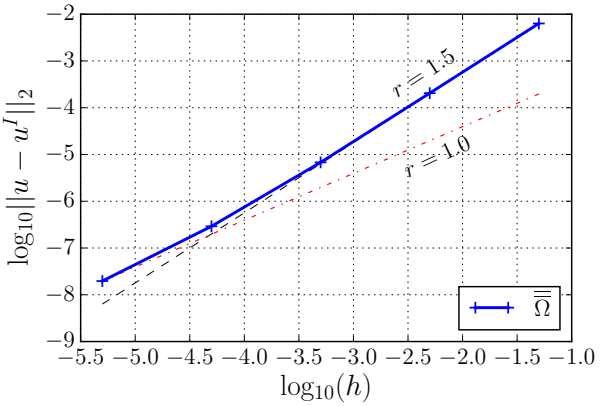

(b) $\epsilon = 2.7h$

Figure 8: Convergence study of approximating $u(x) = e^x$ using constant RK basis with support sizes $\epsilon = 1.7h$ and $\epsilon = 2.7h$. Cubic B-spline is the window function.

8. Conclusion

In this work, the super-convergence of RK approximation are analyzed. We borrowed the idea from [10] and look at error estimates in the entire do-

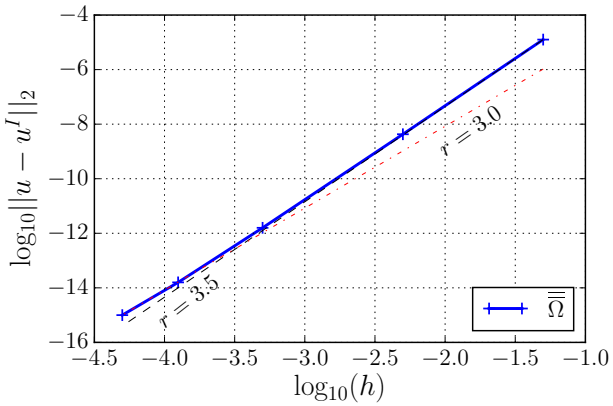

Figure 9: Convergence study of approximating $u(x) = e^x$ using quadratic RK basis with support sizes $\epsilon = 3.7h$. Cubic B-spline is the window function.

main. The key idea is to divide the domain $\overline{\overline{\Omega}}$ into two parts, the interior (Ω) and the boundary (Ω_{bl}), and investigate the approximation errors on them separately. We provide the interpolation error analysis in Sobolev spaces for both the continuous RK approximation and the discrete RK approximation. While the super-convergence always exists for the even order continuous RK approximation as result of the symmetry of window functions, the discrete RK approximation can only be super-convergent with uniform particle distribution and carefully tuned parameters, since the symmetry is not guaranteed with arbitrary distributed particles. Our result is a general one that holds true for multi-dimensional RK approximation.

For general RK support size, error estimates in [5, 10] do not expect super-convergence but numerical experiments have observed higher convergence rates. We call it pseudo-super-convergence and then further explained the pseudo-super-convergence phenomena in many numerical experiments apart from the proven cases in our theorem. In those cases, the observed convergence rates have a clear drop from higher to lower ones along with the mesh refinement. Therefore the pseudo-super-convergence is merely a numerical artifact results from insufficient mesh refinement. However, the transition of convergence rates happens at smaller grid size h if the ratio between RK support size ϵ and h is set to be larger, making the drop of convergence rates hard to be seen in practice. This is understandable because increasing the ratio of ϵ over h makes the discrete RK approximation closer to its corresponding continuous RK approximation, which we know is always super-convergent.

Note that our super-convergence analysis differs from the synchronized convergence introduced in [10, 11] in the way that we are interested in the super-convergence phenomenon of even order RK interpolation in Sobolev norms over the entire domain of interest, while the synchronized convergence phenomenon investigates cases when convergence rates in L^2 norm and higher order norms become the same for some interpolation orders in the interior of the domain. We leave the synchronized convergence in more general RK interpolation order for future work. Finally, we remark that our work involves only interpolation error analysis. The further study of applying the result for solving nonlocal problems is in the separate work [19].

Acknowledgements

The research of Yu Leng and John T. Foster is supported in part by the AFOSR MURI Center for Material Failure Prediction through Peridynamics (AFOSR Grant NO. FA9550-14-1-0073). The research of Xiaochuan Tian is supported in part by the U.S. NSF grant DMS-1819233.

References

[1] S. Brenner and R. Scott, *The mathematical theory of finite element methods*, vol. 15, Springer Science & Business Media, 2007.

[2] I. Daubechies, A. Grossmann, and Y. Meyer, *Painless nonorthogonal expansions*, Journal of Mathematical Physics, 27 (1986), pp. 1271–1283.

[3] T. Dupont and R. Scott, *Polynomial approximation of functions in sobolev spaces*, Mathematics of Computation, 34 (1980), pp. 441–463.

[4] W. Han and W. Liu, *Flexible pievewise approximations based on partition of unity*, Advances in Computational Mathematics, 23 (2005), pp. 191–199.

[5] W. Han and X. Meng, *Error analysis of the reproducing kernel particle method*, Computational Methods in applied mechanics and engineering, 190 (2001), pp. 6157–6181.

[6] R. Jia and J. Lei, *A new version of the strang-fix conditions*, Journal of Approximation Theory, 74 (1993), pp. 221–225.

[7] J.S. Chen, C. Pan and C.T. Wu, *Large deformation analysis of rubber based on reproducing kernel particle method*, Computational Mechanics, 19(3) (1997), pp. 211–227.

[8] J.S. Chen, C. Pan, C.-T. Wu and W.K. Liu, *Reproducing kernel particle methods for large deformation analysis of non-linear structures*, Computer methods in Applied Mechanics and Engineering, 139 (1996), pp. 195–227.

[9] J.S. Chen, C. Pan, C.M.O.L Roque and H.P. Wang, *A Lagrangian reproducing kernel particle methods for metal forming analysis*, Computational Mechanics, 22 (1998), pp. 289–307.

[10] S. Li and W. Liu, *Moving least-square reproducing kernel method part ii : Fourier analysis*, Computational Methods in applied mechanics and engineering, 139 (1996), pp. 159–193.

[11] S. Li and W. Liu, *Synchronized reproducing kernel interpolant via multiple wavelet expansion*, Computational Mechanics, 21 (1998), pp. 28–47.

[12] S. Li and W. Liu, *Reproducing kernel hieratchical partition of unity, part i - formulation and theory*, International journal for numerical methods in engineering, 45 (1999), pp. 251–288.

[13] S. Li and W. Liu, *Reproducing kernel hieratchical partition of unity, part ii - application*, International journal for numerical methods in engineering, 45 (1999), pp. 289–317.

[14] M. Passetto, Y. Leng, J.S. Chen, J.T. Foster, and P. Seleson , *A reproducing kernel enhanced approach for peridynamic solutions*, Computational Methods in applied mechanics and engineering, 340 (2018), pp. 1044–1078.

[15] S. Jun, W. K. Liu, and T. Belytschko, *Explicit reproducing kernel particle methods for large deformation problems*, International Journal for Numerical Methods in Engineering, 41(1) (1998), pp. 137–166.

[16] I. J. Schoenberg, *Contributions to the problem of approximation of equidistant data by analytic functions: Part A. - On the problem of smoothing or graduation. A first class of analytic approximation formulae*, Quarterly of Applied Mathematics, 4(1) (1946), pp. 45–99.

[17] W.K. Liu, S. Jun and Y.F. Zhang, *Reproducing kernel particle methods*, International Journal for Numerical Methods in Fluids, 20 (1995), pp. 1081–1106.

[18] W.K. Liu, S. Li and T. Belytschko, *Moving least-square reproducing kernel methods (i) methodology and convergence*, Computational Methods in applied mechanics and engineering, 143 (1997), pp. 113–154.

[19] Y. Leng, X. Tian, and J.T. Foster, *Convergence analysis of reproducing kernel collocation method for linear nonlocal models*, (in preparation).